scientific reports

Check for updates

OPEN

A bacteriolysin of *Lactococcus carnosus* is potentially involved in mediating contact-dependent antagonism against *Listeria monocytogenes*

Raouf Tareb[1], Sandrine Rezé[1], Manar Harb[1], Laurence Dubreil[2], Veronique Monnet[3], Johanna Björkroth[4], Delphine Passerini[5], Francoise Leroi[5] & Marie-France Pilet[1]✉

Lactococcus carnosus **CNCM I-4031 is a psychrotrophic lactic acid bacterium used for the biopreservation of seafood. It effectively inhibits the growth of spoilage and pathogenic bacteria, such as *Listeria monocytogenes*, through an atypical mechanism that relies on direct cell-to-cell contact, without producing conventional antimicrobial compounds like diffusible bacteriocins, which are released into the environment to eliminate nearby cells during interbacterial competition. However, the precise molecular mechanism behind this bacterial interaction remains to be fully understood. In this study, Label-free LC–MS/MS shotgun proteomics and gene expression analysis were used to examine cell envelope protein expression in *L. carnosus* when cultivated alone and in co-culture with *L. monocytogenes*. The investigation identified a specific cell wall protein, named LYSO, which has a toxic C-terminal domain and demonstrates peptidoglycan hydrolysis activity against *L. monocytogenes*. Further analysis using knockout mutants provided additional evidence for the involvement of LYSO in the inhibition activity. These findings suggest the significant role of this bacteriolysin in the contact-dependent mechanism of *L. carnosus* against *L. monocytogenes*.**

Keywords Lactic acid bacteria, Contact-dependent inhibition, Bacteriolysin, Peptidoglycan hydrolase, Anti-*listeria*

Bacterial ecosystems within food are highly diverse, featuring an array of microorganisms, including spoilage bacteria, foodborne pathogens, and those contributing positively to product quality. When different strains of bacteria coexist in the same environment, their interactions can lead to various outcomes, such as neutralism, commensalism, mutualism, amensalism, and competition[1]. These interactions have significant implications for the overall quality of food products. Notably, amensalism, which refers to the suppression of one bacterial species by another without any reciprocal effect, has received extensive attention in the study of Lactic Acid Bacteria (LAB) to identify strains with significant potential in inhibiting unwanted spoilage bacteria and foodborne pathogens across various food products[2].

Listeria monocytogenes is of particular concern among foodborne pathogens due to its ability to withstand challenging conditions in the food production chain and cause listeriosis, one of the most severe foodborne diseases[3]. This ubiquitous pathogen has been isolated from a large variety of foodstuffs and is particularly of concern in ready-to-eat (RTE) food. *L. monocytogenes* is a major risk for the consumers and the food industry with an alarming mortality rate (20%–30%) for infected humans[3,4]. Ready-to-eat (RTE) foods are generally treated with hurdle technologies to limit the growth of *L. monocytogenes*, including refrigeration, vacuum or modified atmosphere packaging, and the use of chemical preservatives. In recent years, consumer demand has shifted toward reducing chemical preservatives, as some are considered potentially harmful to health. To meet these requirements, there has been a growing focus on milder and healthier biological preservation methods,

[1]Oniris, INRAE, SECALIM, Nantes, France. [2]Oniris, INRAE, APEX, PAnTher, Nantes, France. [3]PAPPSO, Micalis Institute, INRAE, AgroParisTech, Université Paris-Saclay, Jouy-en-Josas, France. [4]Department of Food Hygiene and Environmental Health, Faculty of Veterinary Medicine, University of Helsinki, Helsinki, Finland. [5]Ifremer, MASAE, Nantes, France. ✉email: marie-france.pilet@inrae.fr

such as the use of natural antimicrobial agents like lactic acid bacteria, bacteriocins, bacteriophages, enzymes, and plant-derived essential oils[5–7].

One promising method is the use of LAB as a bioprotective agent, which has demonstrated substantial potential in enhancing food safety and stability[5]. However, it is crucial to understand their interaction mechanisms with target microorganisms to apply LAB effectively. This understanding must consider both biotic and abiotic factors associated with the food matrix, as well as the production and preservation processes[6]. Historically, the inhibitory mechanisms of LAB have been primarily associated with nutritional competition and the production of diffusible organic acids and bacteriocins[7,8]. Bacteriocins, a specific class of antimicrobial peptides, are released by bacteria and act from a distance to harm susceptible cells, providing a competitive advantage to the producing bacteria[9,10]. By comprehensively understanding these mechanisms, we can optimize the efficiency of LAB as bioprotective agents, ensuring safer and more stable food products.

Lactococcus piscium CNCM I-4031, renamed *Lactococcus carnosus* CNCM I-4031[11], a psychrotrophic lactic acid bacterium, has emerged as a promising bioprotective strain for seafood products[12,13]. This strain has demonstrated the ability to improve cooked shrimp's sensory quality and microbial safety by inhibiting the growth of *Brochothrix thermosphacta*[14] and *L. monocytogenes* [15], respectively. Recent studies have highlighted the competitiveness of *L. carnosus* strains and their capacity to significantly reduce the growth of various spoilage and foodborne pathogenic bacteria, including gram-negative and gram-positive species[16]. However, the antimicrobial mechanism employed by *L. carnosus* against different pathogens and spoilage organisms still need to be fully understood. Notably, recent research has revealed that the inhibitory effect of *L. carnosus* CNCM I-4031 on *L. monocytogenes* is not mediated by the release of diffusible antimicrobial compounds (such as known bacteriocins) or nutritional competition, as commonly observed in LAB interactions. Instead, it depends on direct cell-to-cell contact[17].

Contact-dependent growth inhibition occurs when a bacterial cell transfers a polymorphic toxin molecule into neighbouring bacterial cells. Previous research has shed light on Gram-negative bacteria's ability to efficiently deliver various antimicrobial toxins to closely related or genetically distinct bacterial species through direct cell-to-cell contact[18]. This delivery of antimicrobial toxins is often facilitated by specialized secretion systems (SS) such as Type 1SS, Type 4SS, Type 6SS, and contact dependant inhibition (CDI) systems[9,10,18–21]. In contrast, there has been relatively limited research exploring the capacity of gram-positive bacteria to deploy interspecies toxins through direct cell-to-cell contact. Nonetheless, instances of such interactions have been documented in bacteria such as *Bacillus subtilis*, *Bacillus megaterium*, *Streptococcus intermedius*, and *L. monocytogenes*[22–25].

This study aims to explore the contact-dependent growth inhibition observed in *L. carnosus* CNCM I-4031 by elucidating its molecular mechanism. To achieve this, we will conduct a comprehensive investigation using label-free LC–MS/MS shotgun proteomics and relative gene expression analysis. In this work, we have investigated the expression of cell envelope proteins in *L. carnosus* CNCM I-4031, both when cultivated in monoculture and when cocultured in contact with *L. monocytogenes*. The analysis enables to identify a significant candidate among the cell wall proteins of *L. carnosus* CNCM I-4031, a putative peptidoglycan hydrolase named LYSO. Further analysis indicates that LYSO exhibits a toxic C-terminal domain and displays peptidoglycan hydrolysis activity against *L. monocytogenes*. Additionally, the characterization of a knockout mutant of the LYSO protein suggests its involvement in the contact-dependent growth inhibition of *L. monocytogenes* by *L. carnosus* CNCM I-4031.

Results

Identification of differentially abundant proteins of *L. carnosus* CNCM I-4031 in the coculture with *L. monocytogenes* relative to the monoculture condition

This study used a proteomic approach to investigate the cell-to-cell contact inhibition mechanism of *L. monocytogenes* ScottA by *L. carnosus* CNCM I-4031. Specifically, we extracted and analyzed cell envelope protein-enriched fractions from three biological replicates of the coculture of *L. carnosus* CNCM I-4031 in contact with *L. monocytogenes ScottA* and compared these with the monoculture of *L. carnosus*. Our analysis revealed 911 proteins for *L. carnosus* CNCM I-4031 under monoculture conditions and 934 under coculture conditions (Fig. S1 and Supplemental file 1). Of these, 780 and 820 proteins were shared in all three biological experiments in monoculture and coculture conditions, respectively (Fig. S1A–B).

Moreover, mutual exclusivity analysis revealed that 737 proteins were shared to both culture conditions, while 43 and 83 proteins were specific to the monoculture and coculture conditions, respectively (Fig. S1C). Thus, 863 proteins were identified in both coculture and monoculture conditions, representing 43% of the predicted ORFs encoded by the *L. carnosus* CNCM I-4031 genome (Table S1). Supplementary Table S1 overviews the predicted localizations of the 863 recovered proteins from *L. carnosus* CNCM I-4031 in both culture conditions. According to the LocateP prediction, 693 (44%) were identified as cytoplasmic proteins, and 170 were predicted to have a cell envelope localization. Among the cell envelope proteins, 85 were integral membrane proteins, and 85 were surface proteins. The results demonstrated notable representation compared to the expected envelope-proteins in the *L. carnosus* CNCM I-4031 genome. After analysis of each independent biological replicate, a final dataset containing only proteins present in all three datasets was generated (Suppl file 1).

To identify differentially abundant proteins between the two experimental conditions, our analysis focused on protein candidates that met stringent criteria, requiring a minimum of two unique peptides and consistent detection in all three biological replicates. This selection ensured a reliable dataset for subsequent analyses. Besides, the samples from each replicate demonstrated robust technical and biological reproducibility, as evidenced by calculating high Pearson correlation coefficients and hierarchical analysis of spectral counts across the comprehensive set of proteins identified in both culture conditions. The results of these analyses are depicted in Supplementary Fig. S2, further validating the consistency and reliability of our experimental approach. Based on a set of statistical criteria (T-test p-value < 0.05 and Log2 "fold change" cutoff point > 2), we highlighted 42

proteins with significantly changed abundance between the two conditions (Fig. 1 A-B and Supplemental file 1). Among these proteins, 27 were significantly more abundant (MA), and 15 were less abundant (LA) in coculture conditions. Regarding the subcellular localization of the 27 MA proteins found in coculture conditions (Table 1), 19 were predicted to have a cytoplasmic localization, and 5 were identified as cell envelope proteins. Among the cell envelope proteins, 3 were predicted to be integral membrane proteins, and 2 were cell surface-exposed proteins (LYSO: SCA91560.1 and PLY: SCA91317.1). The MA proteins were categorized into biological process categories as defined by GO AND KEGG databases (Table 1). They were mainly classified into various functional groups, including amino acid (4), purine (3), lipid (3), and carbohydrate (3) transport and metabolism. The remaining identified proteins were categorized as transcriptional regulators (4), proteins of unknown function (4) or associated with DNA recombination and repair (3), and plasmid replication and mobilization (3). Of particular interest, two cell surface-exposed proteins (SCA91560.1 and SCA91317.1) were identified as potential candidates involved as effectors in cell-to-cell contact growth inhibition. The SCA91317.1 protein did not reveal any known functional domains, except for a peptidoglycan-binding lysin (LysM) domain in its N-terminal region. Conversely, the SCA91560.1 protein was predicted to belong to bacterial peptidoglycan hydrolases, harboring a C-terminal Lysozyme-like domain. Given their characteristics, these proteins appear to be potential candidates for the role of cell-to-cell contact growth inhibition effectors in *L. carnosus*. Consequently, SCA91560.1 and SCA91317.1 were designated as LYSO and PLY, respectively.

Gene expression analysis of the more abundant cell surface proteins LYSO and PLY

We determined the transcriptional level of genes encoding LYSO and PLY protein of *L. carnosus* by quantitative reverse-transcription polymerase chain reaction under comparable experimental conditions described above (coculture and monoculture at 25 h). The transcription levels of *lyzo* and *ply* genes in coculture were quantified as fold changes relative to monoculture, with normalization to the reference *recA* and *rpoB* gene transcription levels. The choice of *recA* for normalization yielded results consistent with those obtained with *rpoB*, as illustrated in the Fig. 2. Similar mRNA expression of *ply* was obtained between the two conditions. However, the transcription level of the *lyzo* gene demonstrated a significant up-regulation (> twofold) in coculture compared to monoculture, aligning seamlessly with the proteomic data. Consequently, integrating proteomic evidence with subsequent qRT-PCR validation affirmed the overexpression of LYSO protein in *L. carnosus* upon coculture with *L. monocytogenes* cells.

Functional characterization of LYSO protein

The in silico analysis predicted that LYSO would encode a protein of 197 amino acids (Fig. 3A) with a deduced molecular mass of 22,230 Da. The N-terminal part of 24 amino acids exhibited all the properties of Gram-positive Sec signal peptide (Sec/SPI) with an identified putative peptidase cleavage site. Furthermore, a transmembrane helix region was predicted between the seventh and the twenty-fourth amino acids. Also, a region of 161 amino acids harboring a Lysozyme_like domain (Pfam PF13702.6) was identified (Fig. 3A). This finding indicates that LYSO is a putative muramidase belonging to the Lyz-like superfamily (cl00222). To examine whether LYSO, possessing a predicted peptidoglycan-degrading activity, could induce the lysis of bacterial cells, toxicity assays

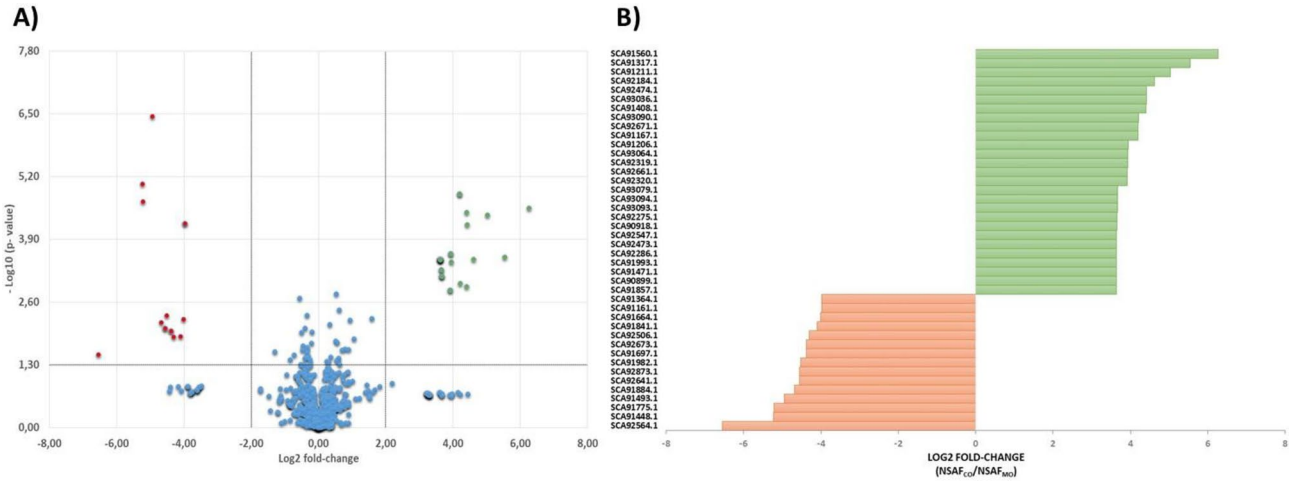

Fig. 1. Label-free proteomics analysis of *L. carnosus* CNCM I-4031 in coculture and monoculture. (**a**) Volcano plot of differentially abundant proteins (t-test $p \leq 0.05$ and log2 fold change cutoff point ± 2) between the coculture and the monoculture condition. Y-axis indicates – Log10 (*p*-value), X-axis shows *L. carnosus* protein abundance ratio in Coculture (CO) vs monoculture (MO). The color code indicates more abundant proteins (green) and low abundant proteins (red). Proteins with no statistically significant difference in abundance between the two conditions are shown in blue. (**b**) The bar chart shows the mean log2 (fold change NSAF coculture/NSAF monoculture) of the proteins abundance of *L. carnosus*. The positive fold changes (green) and the negative fold changes (red), indicate respectively the more abundant (MA) proteins and the less abundant (LA) proteins observed in the coculture condition.

ID	Description	Biological process	Molecular function	Cellular destination
SCA91471.1	Conserved hypothetical protein		Unk	Unk
SCA93036.1	Conserved hypothetical protein		Unk	Unk
SCA91317.1	Putative lysozyme or peptidoglycan lyase containing peptidoglycan-binding lysin domain	Unk	LysM domain	Surf
SCA91560.1	Lytic murein transglycosylase family (Lysozyme like)		Lysozyme-like [E:C:3.2.1.14; EC:3.2.1.17]	Surf
SCA92671.1	Putative transcriptional regulator		DNA binding	Cyto
SCA92286.1	putative transcriptional regulator, LysR family	Regulation of DNA-templated transcription	DNA binding; DNA-binding transcription factor activity	Cyto
SCA92661.1	Putative transcriptional regulator		DNA binding	Cyto
SCA93079.1	Ribose operon repressor		DNA binding	Cyto
SCA93090.1	Putative bacterial Mobilization protein mobC		MobC-like: belong to the group of relaxases	Unk
SCA93093.1	Adenosine monophosphate-protein transferase, fic (filamentation induced by cAMP)domain	Plasmid replication & mobilization	AMPylase activity	Cyto
SCA93094.1	Putative replication initiator protein, RepB		DNA-directed DNA polymerase activity	Cyto
SCA92319.1	N5-carboxyaminoimidazole ribonucleotide mutase		Isomerase activity; purE; [EC:5.4.99.18]	Cyto
SCA91857.1	Phosphoribosylaminoimidazole synthetase	Purine transport & metabolism	Phosphoribosylformylglycinamidine cyclo-ligase activity; purM; [EC:6.3.3.1]	Cyto
SCA92320.1	Phosphoribosylamine--glycine ligase		Phosphoribosylamine-glycine ligase activity; ATP binding; metal ion binding; [EC:6.3.4.13]	Cyto
SCA90899.1	Phosphatidate cytidylyltransferase (CDP-diglyceride synthase)		Transferase activity, transferring phosphorus-containing groups; [EC:2.7.7.41]	Memb
SCA90918.1	Putative Glycerophosphoryl diester phosphodiesterase (GLPQ, YQIK)	Lipid transport & metabolism	Phosphoric diester hydrolase activity; [EC:3.1.4.46]	Cyto
SCA91408.1	Putative 3-oxoacyl-acyl carrier protein reductase		Oxidoreductase activity; fabG; [EC:1.1.1.100]	Cyto
SCA91167.1	Holliday junction resolvase		Nuclease activity; ruvX; [EC:3.1.-.-]	Cyto
SCA91206.1	Holliday junction ATP-dependent DNA helicase RuvA	DNA recombination & repair	DNA helicase activity; ATP binding; four-way junction helicase activity; DNA binding; ruvA [EC:3.6.4.12]	Cyto
SCA91211.1	ATP-dependent DNA helicase, component of RuvABC resolvasome		ATP binding; DNA binding; four-way junction helicase activity; ATP hydrolysis activity; ruvB; [EC:3.6.4.12]	Cyto
SCA92474.1	PTS system, trehalose-specific IIB component		Trehalose transmembrane transporter activity; [EC:2.7.1.201]	Memb
SCA92473.1	Trehalose-6-P hydrolase / GH13, similar to LACPI-1657 from L. piscium MKFS47	Carbohydrate transport & metabolism	Alpha,alpha-phosphotrehalase activity; treC; [EC:3.2.1.93]	Cyto
SCA92275.1	Glucan 1,6-alpha-glucosidase / GH13, similar to LACPI-1446 from L. piscium MKFS47		Alpha-amylase activity; Dextran glucosidase; [EC:3.2.1.70]	Cyto
SCA92547.1	Glutamate and aspartate transporter subunit; ATP-binding component of ABC superfamily		ATP binding; ATP hydrolysis activity; ABC-type amino acid transporter activity; ABC.GLN1.A; [EC:3.6.3.-]	Memb
SCA91993.1	Glutamate racemase	Amino acid transport & metabolism	Glutamate racemase activity; murI; [EC:5.1.1.3]	Cyto
SCA92184.1	Arginine biosynthesis bifunctional protein ArgJ		Glutamate N-acetyltransferase activity; [EC:2.3.1.35, EC:2.3.1.1]	Cyto
SCA93064.1	Imidazoleglycerol-phosphate dehydratase		imidazoleglycerol-phosphate dehydratase activity; hisB; [EC:4.2.1.19]	Cyto

Table 1. Subcellular distribution and biological process classification of the more abundant (MA) proteins in the coculture condition.
Unk: Unknown, Surf: Surfaceome, Memb: Membranome, Cyto: Cytoplasmic.

were conducted in *Escherichia coli*. We hypothesized that if LYSO is transported in the periplasmic compartment in direct contact with peptidoglycan, it might induce the lysis of *E. coli* cells. To address this inquiry systematically, we employed a cloning strategy to insert the sequence region containing the Lysozyme_like domain of the LYSO gene into two distinct plasmids: pET100 for cytoplasmic expression and pET22b (designated as Peri-LYSO and equipped with the pelB signal peptide) for targeting the protein to the periplasm (Fig. 3B). Subsequently, these recombinant plasmids were introduced into the *E. coli* host. As anticipated for a peptidoglycan-degrading enzyme, the artificial targeting of LYSO to the periplasm through a sec-dependent leader sequence (peri-LYSO) resulted in a significant decrease in *E. coli* viability and optical density. Conversely, the expression of LYSO in the cytoplasm of *E. coli* was notably better tolerated (see Fig. 3C, D). Time-lapse microscopy further revealed that

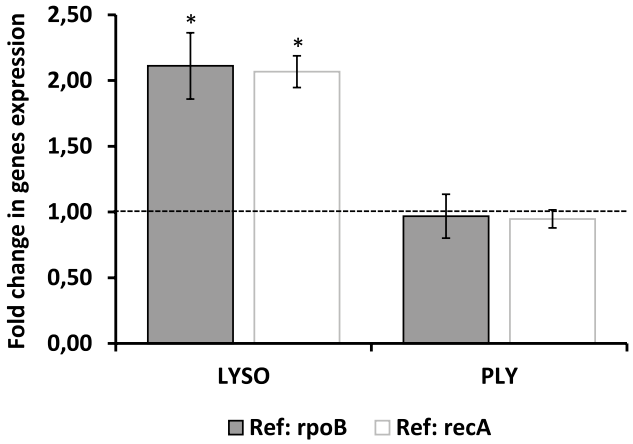

Fig. 2. Effect of coculture with *L. monocytogenes* Scott A on the expression of *L. carnosus* CNCM I-4031 LYSO and PLY encoding genes. The coculture and monoculture of ***L. carnosus*** CNCM I-4031 were conducted in MSMA broth at 26 °C for 25h. Fold change in mRNA expression of target genes was determined using Real-Time Quantitative PCR and the $2^{-\Delta\Delta CT}$ Method. Growth of the CNCM I-4031 strain in monoculture was used as a control. Expression levels were normalized against the reference genes *rpoB* and *recA*. Error bars represent SD from three replicates and * $p < 0.05$.

periplasmically localized forms of LYSO proteins (peri-LYSO) induced cell rounding and prompt cell lysis upon induction (Fig. 3E and Supplemental file 2).

To assess the cell wall hydrolytic activity of LYSO against *L. monocytogenes*, the recombinant 6-His tagged LYSO protein, lacking the signal peptide (Sec/SPI), was synthesized in *Escherichia coli* Lemo21(DE3) utilizing the pET 100/D-TOPO plasmid. Subsequently, the 6-His tagged protein was purified using NEBExpress Ni Spin Columns. Analysis through SDS-PAGE and Western Blot, employing anti-6xHis tag antibodies, revealed that the purified His-LYSO migrated as a 25 kDa protein (Fig. 4A, B). Afterwards, zymogram gels were employed to assess enzymatic activity, with *L. monocytogenes*, *L. carnosus*, or *Micrococcus lysodeikticus* cells serving as substrates. In the zymogram assay using *M. lysodeikticus* cells (suitable substrate for the detection of the bacteriolytic enzyme), distinct clearance bands were observed at 25 kDa and 14 kDa, corresponding to the lytic activity of the purified recombinant LYSO (3 µg) and the commercial lysozyme used as a positive control (3 µg), respectively (Fig. 4C). Notably, the zymogram experiments demonstrated that the recombinant LYSO also functions as a cell wall hydrolytic enzyme against *L. monocytogenes* (Fig. 4D), with no detectable activity observed for *L. carnosus* under the same assay conditions (data not shown). In summary, these results establish that LYSO exhibits peptidoglycan-degrading enzymatic activity, also targeting *L. monocytogenes* in a zymogram assay.

To assess the implication of the LYSO protein in contact-dependent inhibition activity (bacterial antagonism), we conducted coculture assays between wild-type (WT) and Δ*LYSO* strains of *L. carnosus* (acting as the "attacker" strain) and *L. monocytogenes* (serving as the "target" strain) (Fig. 5A). In the cell–cell contact conditions, *L. carnosus* strains and *L. monocytogenes* were cocultured together in the same well, allowing for extensive and direct cell–cell interactions. This setup substantially reduced the number of recovered target cells (*L. monocytogenes*) compared to non-cell–cell contact conditions, where the attacker and target strains were cocultured in separate compartments using a transwell system as previously. However, the disruption of the LYSO gene led to a significant reduction in inhibitory activity, although it did not altogether abolish it. The number of recovered target cells in contact with the mutant strain increased tenfold compared to the coculture condition in contact with a wild-type attacker (Fig. 5B). These findings indicate that the LYSO gene plays a role in the observed bacterial antagonism, emphasizing its contribution to the inhibitory effects during direct cell–cell interactions between *L. carnosus* and *L. monocytogenes*.

Discussion

The inhibition observed in LAB with anti-*Listeria* activities suitable for biopreservation generally involves classical mechanisms such as the production of bacteriocins and competition[6]. Recent research has revealed that the *L. carnosus* CNCM I-4031 can prevent the growth of *L. monocytogenes* using a cell-to-cell contact-dependent mechanism[17]. This study provides a comprehensive exploration of the contact-dependent growth inhibition (CDI) mechanism observed in *L. carnosus* CNCM I-4031 when interacting with *L. monocytogenes*. Using label-free LC–MS/MS shotgun proteomics and relative gene expression analysis, we identified a key candidate among the cell wall proteins of *L. carnosus* CNCM I-4031: a putative peptidoglycan hydrolase named LYSO. This protein, predicted to be secreted via a sec-dependent pathway, contains a Lysozyme-like domain in the C-terminal region and exhibits peptidoglycan hydrolysis activity against *L. monocytogenes*. The knockout mutant of LYSO confirmed its role in CDI. Peptidoglycan hydrolases are a diverse group of enzymes with different origins but similar structural characteristics. They target peptidoglycan, an essential component of bacterial cell walls. By disrupting the cell wall, they cause bacterial cell lysis and play crucial roles in various physiological processes

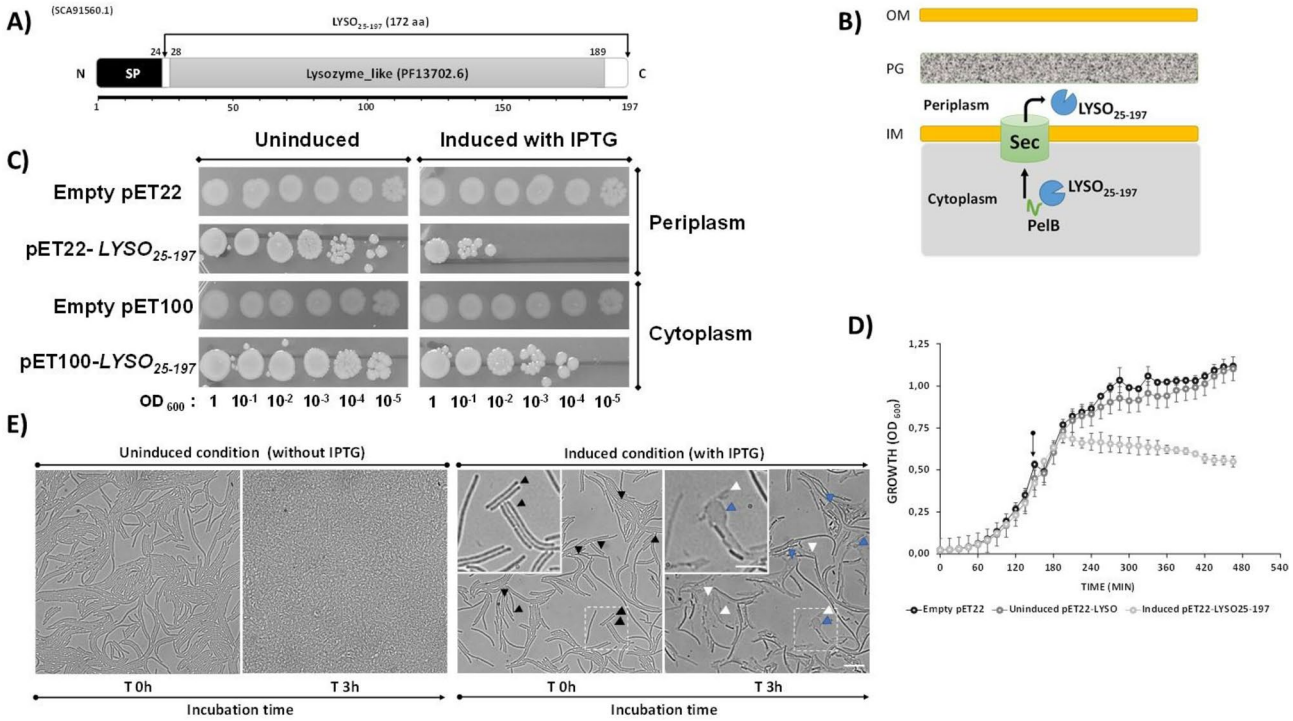

Fig. 3. Directed export of $LYSO_{25\text{-}197}$ protein to the periplasm of *E. coli* is toxic and results in cell lysis. (**A**) Schematic of the domain and motif organization of the LYSO protein (SCA91560.1). The black box indicates the signal peptide (SP) located within the protein's N-terminal amino acids 1 to 24. The gray box indicates 161 amino acids of the Lysozyme_like domain (Pfam PF13702.6). Domains, motifs, and amino acid positions were assigned with Interproscan, SMART, and SignalP 5.0. Numbers indicate the amino acid positions. The indicated 172 amino acid represents the segment expressed in *E. coli* (From the 25th to the 197th aa). (**B**) Schematic representation of the toxicity experiments in (**C**). IM, inner membrane; OM, outer membrane; PG, peptidoglycan; PelB, signal peptide. (**C**) Gene encoding *L. carnosus* CNCM I-4031 LYSO protein was heterologously expressed in the cytoplasm or periplasm compartment of *E. coli* Lemo21 using pET100 or pET22 plasmid, respectively. For pET22, periplasmic localization was achieved by fusion the PelB leader sequence at the N-terminus of the LYSO protein. Serial dilutions of *E. coli* strains were spotted on LB media plates, and gene expression was induced with IPTG. The used vectors are indicated on the left, and the density of the inoculum is given at the bottom of the images. The empty vectors were used as a negative control. Plates were incubated at 37 °C for 18 h, after which they were photographed. (**D**) Growth curves of *E. coli* Lemo21 harboring indicated plasmids were obtained by measuring OD_{600} at 15 min intervals. Cultures were induced at the indicated time (arrow) with IPTG. Error bars indicate ± s.d. (n = 3). (**E**) Representative micrographs of *E. coli* Lemo21harboring pET22-$LYSO_{25\text{-}197}$ grown on LB agar pads under uninduced (without IPTG) and induced (with IPTG) conditions. Cells were spotted on LB agar pads, and images were acquired at T0 and T3h. Black arrowheads indicate intact bacterial cells at T0. Blue arrowheads indicate cell rounding, and white arrowheads point to lysed cells observed at T3h in the presence of IPTG. Scale bar: 10 µm (full image); 5 µm (inset, dotted white area).

throughout the bacterial life cycle. These enzymes, especially endolysins, are important components of the bacteriophage lytic arsenal. They also play roles in peptidoglycan remodeling and degradation (autolysins) or in competitive interactions among closely related bacterial strains[26,27]. For example, Class III bacteriocins comprise large peptides (Mr ≥ 25 kDa), which are generally heat-labile antimicrobial proteins with enzymatic bactericidal activity targeting the bacterial cell wall. These proteins, known as bacteriolysins, include Enterolysin A, zoocin A, millericin B, bacteriocin 41, stellalysin, and lysostaphin[28–31]. They act by cleaving the peptidoglycan present in the cell walls of sensitive bacteria.

Many of bacteriolysins harbor an N-terminal Sec signal sequence and are translated as preproteins to be secreted by the Sec pathway like LYSO protein. The N-terminal Sec signal peptide, which consists of positively charged residues at the N-terminus, a hydrophobic core, and a polar C-terminal cleavable site, is recognized by the Sec-dependent secretion machinery[32]. For example, mature enterolysin A (EnlA) is a class III heat-labile bacteriocin of 316 amino acids, synthesized by *Enterococcus faecalis* as a 343 amino acid preprotein with a Sec-dependent peptide of 27 amino acids. This mature bacteriocin breaks down the cell wall of Gram-positive bacteria, including sensitive *Lactococcus lactis*[31,33].

However, contrary to our observations regarding the killing mechanism of LYSO, previously studied bacteriolysins from lactic acid bacteria have not been reported to exhibit a contact-dependent inhibition (CDI) mechanism. Our data suggest that LYSO remains associated with the surface of the producing cell

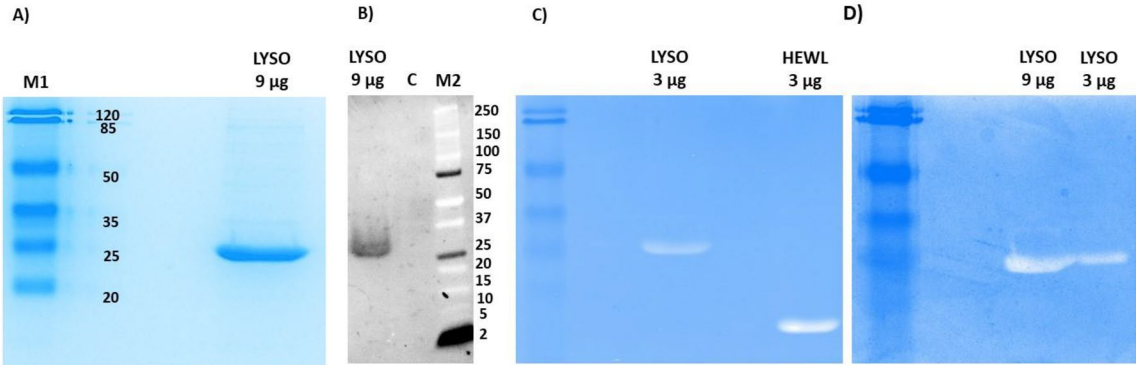

Fig. 4. The lytic activity detection of LYSO protein against *Micrococcus lysodeikticus* and *Listeria moncytogenes* cell walls. (**A**) SDS-PAGE analysis and (**B**) cropped representative Western blot image showing detection of the 6xHis-tagged $LYSO_{25–197}$ protein used for the zymogram assay, following purification with NEBExpress Ni Spin Columns. A protein band of approximately 25 kDa, corresponding to the recombinant 6xHis-tagged $LYSO_{25–197}$, was observed. Electrophoresis was performed using a 12.5% SDS-PAGE gel. For Western blot analysis, the negative control (**C**) and 9 µg of the purified protein were loaded. Resolved proteins were transferred onto a nitrocellulose membrane and probed using an Anti-6xHis Tag Mouse Monoclonal Antibody (MA1-21315-HRP). Chemiluminescent detection was performed using the SuperSignal™ West Pico PLUS Chemiluminescent Substrate (34577). Protein markers: M1, Pierce Prestained Protein MW Marker (26612, Life Technologies); M2, Precision Plus Protein™ Dual Xtra Prestained Marker. The full-length blot is available in Supplementary Fig. S7. (**C**, **D**) Zymogram analysis showing peptidoglycan hydrolase activity of the purified 6x-His-tagged $LYSO_{25-197}$ protein against (**C**) *Micrococcus lysodeikticus* and (**D**) *Listeria moncytogenes* ScottA. Hen Egg-White Lysozyme (HEWL) was used as a positive control. The zymogram gels contained 0.2% (wt/vol) of autoclaved *Listeria monocytogenes* cells or *Micrococcus lysodeikticus* cells (M0508, Sigma) as substrate. The amounts of each protein loaded are indicated (in µg) above each lane.

and is delivered locally upon physical contact. This hypothesis aligns with other known examples of contact-dependent bacteriocin systems, such as the CdzC/CdzD system from the gram-negative bacterium *Caulobacter crescentus* and the Listeriolysin S (LLS) system from the gram-positive bacterium *Listeria monocytogenes*. Both systems require direct cell contact to mediate their antimicrobial activity[24,34]. For instance, Listeriolysin S (LLS) is a thiazole/oxazole–modified microcin (TOMM) produced by hypervirulent strains of *L. monocytogenes*. It remains localized to the bacterial cell membrane of LLS-producing bacteria and exerts its killing mechanism through direct contact with target bacteria, impairing their membrane integrity and inducing membrane depolarization[24]. Meanwhile, the two-peptide bacteriocin CdzC/CdzD from *C. crescentus* forms insoluble aggregates that are retained on the outer membrane of producer cells. This bacteriocin utilizes an adhesion system encoded elsewhere in the genome and displays a CDI mechanism against other gram-negative bacteria[34]. These findings highlight the existence of contact-dependent bacteriocin delivery in gram-positive and gram-negative bacteria, emphasizing the importance of these interactions in interspecies bacterial competition.

Disruption of the ***lyso*** gene significantly reduced inhibitory activity, although it was not completely abolished. This observation indicates that LYSO contributes to bacterial antagonism during direct cell-to-cell interactions while suggesting additional antimicrobial effectors' involvement in the overall inhibitory mechanism. It is well-established that many bacteria produce multiple lytic bacteriocins and that antimicrobial factors often act in synergy to maximize their effects. For example, in *Streptococcus pneumoniae*, effective allolysis requires the combined action of bacteriocins and murein hydrolases (CbpD, LytA and LytC). ComX-dependent murein hydrolase choline-binding protein D (CbpD) is a key effector in pneumococcal cell lysis, creating specific cleavages in peptidoglycan peptide stems that enable other hydrolases (N-acetylmuramoyl-L-alanine amidase LytA and lysozyme LytC) to act synergistically, enhancing cell lysis beyond CbpD's individual activity. While CbpD expression is strictly competence-dependent, lytA transcription responds to multiple stimuli, including competence, and lytC expression remains constant regardless of competence state[35,36]. Although *ply* gene expression in *L. carnosus* does not appear to change during co-culture with *L. monocytogenes*, this result is inconsistent with the proteomic data, suggesting potential post-transcriptional regulation. The possible role of the PLY protein in antimicrobial activity, particularly its potential synergy with the lytic action of the bacteriolysin LYSO described in this study, warrants further investigation. This hypothesis is supported by well-characterized models in *Streptococcus* and *Enterococcus* species, where the coordinated activity of hydrolases, under both constitutive and inducible regulation, leads to optimized cell lysis.

Furthermore, a recent *in silico* analysis of the *L. carnosus* CNCM I-4031 genome revealed the presence of a locus encoding a type VIIb secretion system (T7SSb), as well as two loci encoding polymorphic antimicrobial toxins belonging to the LXG family of proteins[11]. LXG effectors are polymorphic toxins secreted by the T7SSb pathway, characterized by a conserved Leu-X-Gly (LXG) motif and bearing a toxic C-terminal domain11. Recent studies have shown that T7SS and its associated LXG effectors play a key role in interbacterial competition, notably by mediating contact-dependent inhibition. This system enables bacteria to establish and persist in complex microbial ecosystems[37–39]. These results suggest a potential synergy between the T7SS-LXG system

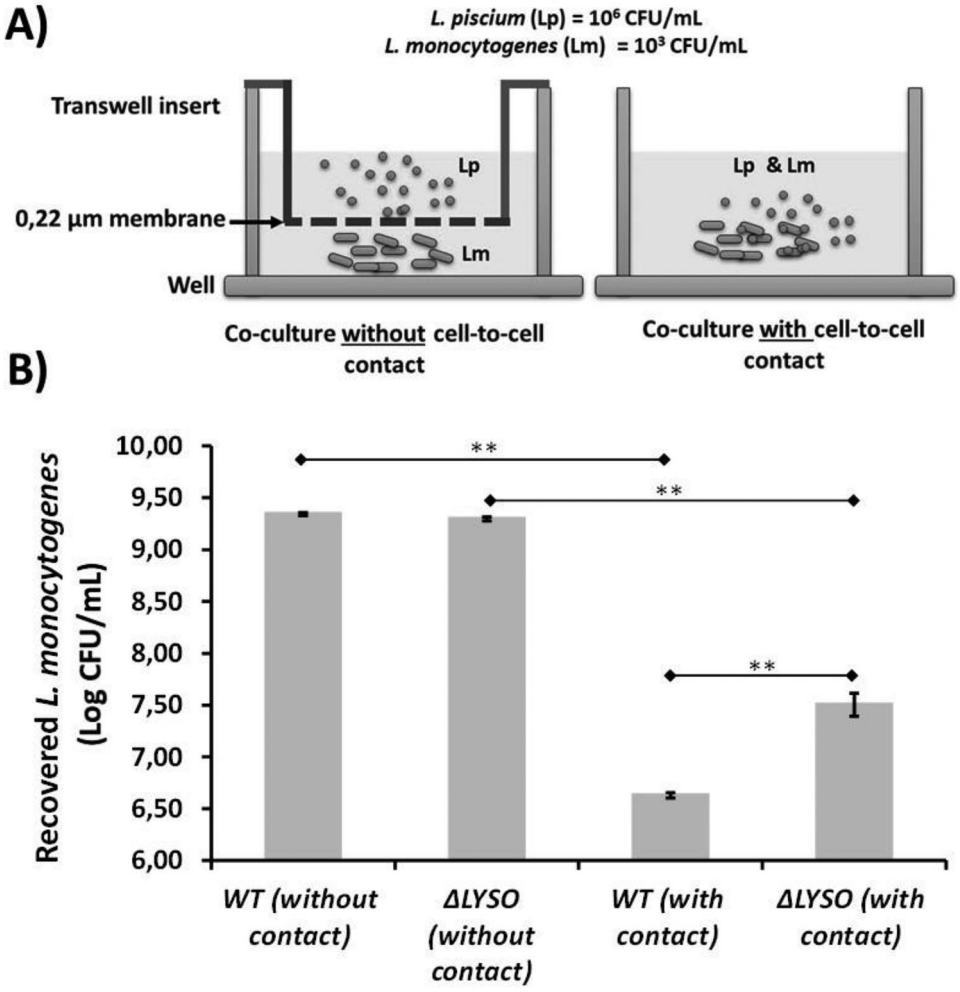

Fig. 5. LYSO protein plays a role in the contact-dependent inhibition activity of *L. carnosus* against *L. monocytogenes*. (**B**) Recovery of viable *Listeria monocytogenes* ScottA following coculture with the CNCM I-4031 wild-type strain (WT) or the isogenic *ΔLYSO* strain. Data are presented as the mean ± SD of three independent experiments. The P-values were determined using a two-tailed unpaired Student's t-test, and differences were acknowledged as statistically significant at $P < 0.05$. (**A**) The experimental setup of the competition assays. Two different modes of coculture system were used. In non-cell-to-cell contact conditions, *L. carnosus* and *L. monocytogenes* Scott A cells were cocultured in two different compartments (insert membrane and well). The medium is shared between the inner and outer compartments, while the cells cannot pass the 0.22 µm membrane barrier. In cell–cell contact conditions, both cells are mixed and cultured on the same well, thus allowing extensive and direct cell–cell interactions. The competition assays were done on the MSMA medium at 26 °C for 25h. Each strain's initial and final populations were enumerated by plating on selective culture conditions.

and the LYSO bacteriolysin identified in this study. This could also explain why contact-dependent inhibition is reduced but not completely abolished in the *lyso* gene mutant.

The production of antimicrobial molecules, like bacteriocins and toxin secretion systems (T4SS, T5SS, T6SS, and T7SS), is tightly regulated by various cellular mechanisms. In Gram-negative bacteria, T6SS facilitates inter-bacterial antagonism by delivering toxins to neighboring cells, with regulation occurring at pre- and post-translational levels[40]. For exemple, in *Pseudomonas aeruginosa*, T6SS assembly is controlled by the kinase PpkA, activated by cell envelope damage from T6SS attacks or other factors[41]. Toxin-specific effectors and signals from quorum sensing and nutrient availability also influence these regulatory processes, enabling bacteria to precisely control toxin production and release for survival and competitiveness[40].

The bacteria that produce bacteriocin or deliver toxins directly to target cells through cell-to-cell contact have specific immunity factors that protect the producer strain from being killed by antimicrobial molecules[42]. In our research, we observed that the peptidoglycan of *L. carnosus* is resistant to the lytic activity of LYSO, indicating an inherent self-protection mechanism. This resistance may be due to the structural modifications of the peptidoglycan to reduce the effectiveness of the bacteriolysin. For example, *Staphylococcus simulans* reduces its susceptibility to lysostaphin by by modifying the amino acid composition of interpeptide chains in cell wall peptidoglycan by increasing the serine content and decreasing the glycine content[43]. Accessory cell wall

polymers like lipoteichoic acid and teichoic acid also act as endogenous inhibitors of peptidoglycan hydrolases[44]. Further research is required to uncover specific self-protection strategies in *L. carnosus*.

In summary, our data indicate that LYSO is a bacteriolytic enzyme involved in countering *Listeria monocytogenes* through the action of *Lactobacillus carnosus* CNCM I-4031. To our knowledge, this is the first bacteriolysin identified in Gram-positive bacteria that is implicated in the CDI (Contact-Dependent Inhibition) mechanism. Further research is required to elucidate how LYSO gains access to target cells and how the LYSO-producing cell protects itself from self-toxicity and damage. In addition, more work is needed to decipher the molecular cascade that triggers LYSO expression upon contact with target cells. This includes investigating the signaling pathways and regulatory networks that mediate LYSO production in response to direct cell–cell interactions. It is also essential to determine whether the PLY and/or TSS7 toxin-antitoxin systems, identified in the *L. carnosus* genome[11], are involved in the CDI mechanism and whether they act synergistically with the bacteriolysin LYSO identified in this study. Understanding these regulatory mechanisms could provide novel insights into the adaptive strategies of *L. carnosus* in competitive microbial environments. Finally, future studies should explore the potential application of LYSO as a bacteriolytic agent for controlling harmful bacteria in the food industry.

Methods

Bacterial strains, culture media, and conditions:

The biopreservative strain of *Lactococcus carnosus* (formerly *L. piscium*) CNCM I-4031 was isolated from fresh salmon steak packed under a modified atmosphere[11]. The food pathogen strain *L. monocytogenes* ScottA (CIP 103575) is a clinical isolate purchased from the Collection of Institute Pasteur (CIP). The genome of *L. carnosus* CNCM I-4031 and *L. monocytogenes* ScottA are available in the NCBI genome database under the accession number NZ_FLZT00000000.1 and AFGI00000000.1 respectively[45,46]. The strains were stored at – 80 °C in their respective culture media supplemented with 20% glycerol (Sigma Aldrich, Saint-Louis, MO, United States). For precultures, *L. carnosus* and *L. monocytogenes* were propagated in Elliker broth (Biokar Diagnostic, Beauvais, France) and Brain heart infusion (BHI) with 2% NaCl (Biokar Diagnostic, Beauvais, France) respectively, for 24 h at 26 °C. The bacterial cultures were diluted in their respective fresh medium to obtain appropriate initial cell concentrations when required. *L. monocytogenes* ScottA was enumerated by surface plating on BHI agar supplemented with 2% NaCl after incubation at 37 °C for 24h. *L. carnosus* CNCM I-4031 cell numbers were estimated by plating on Elliker agar plates incubated at 8 °C for 5 days under anaerobic conditions. For monoculture and coculture experiments, the MSMA (Modified Shrimp Medium A) medium was prepared according to the description of Saraoui et al.[17].

Mono and coculture experiments

Mono and coculture experiments were performed according to the method described by Saraoui et al.[17]. Briefly, coculture and monoculture were achieved in an Erlenmeyer flask containing 400 ml of sterile MSMA medium. *L. carnosus* CNCM I-4031 and *L. monocytogenes* were co-inoculated at 10^6 CFU/mL and 10^3 CFU/mL in the MSMA medium, respectively. A monoculture of each strain was performed as a control. The flasks were incubated at 26 °C for 25 h, and each experiment was performed in triplicates. The incubation time for cell envelope analysis (25h) represents the time when the growth inhibition of *L. monocytogenes* by *L. carnosus* reaches its maximum[17]. At times 0h and 25h, *L. monocytogenes* and *L. carnosus* CNCM I-4031 enumerations were performed as described above to monitor the growth of both strains in different culture conditions and to check the inhibition effect.

Extraction of a fraction enriched in cell envelope proteins

The fractions enriched in cell envelope proteins of coculture and monoculture-grown cells were obtained using a protocol adapted from Gitton et al.[47]. Briefly, bacterial pellet was recovered by centrifugation at 12 000 × g for 5 min at 4 °C and resuspended to 80 OD_{600nm} /ml (160 mg/mL) in 5 ml of Lysis buffer [20 mM sodium phosphate buffer, pH 6.4, 1 X of Protease Inhibitor Cocktail (Sigma-Aldrich), 60 U/mL catalase (Sigma-Aldrich) 10 mM tributylphosphine (Sigma-Aldrich)] maintained at 4 °C.

After a washing step, the suspended cells were mechanically disturbed with a sonicator (Vibracell 72434, Bioblock Scientific, France). The sonications were done using the following parameters: 50W, 15 cycles, 15 s on/15 s off at 4 °C. The suspension was centrifuged at 5,000 g for 20 min at 4 °C to remove unbroken cells and large cellular debris. The supernatants were collected and subjected to ultracentrifugation at 200,000 g for 30 min at 4 °C to separate the "fraction enriched in cell envelope pellets" from exclusively soluble cytosolic proteins. Finally, the pellets were resuspended in the lysis buffer and sonicated for 15 min at 4 °C in an ultrasonic bath. Protein extracts were prepared for each condition (coculture and monoculture) in three independent experiments. Protein concentration was determined using the Pierce BCA Protein Assay Kit (Thermo Fisher Scientific, France).

Gel-based nano–liquid chromatography-tandem mass spectrometry

In-gel digestion and sample preparation

Twenty micrograms of resuspended cell-envelope proteins were solubilized in 20 µL of 6% glycerol, 50 mM DTT, 2% SDS, 75 mM Tris, pH 6.8, 0.1% bromophenol blue (final concentrations) by sonication for 15 min at 4 °C in an ultrasonic bath. The proteins were then separated by denaturing SDS-PAGE on 4 – 15% polyacrylamide mini gels (mini-PROTEAN, Bio-rad, France) in 1× of TGS buffer (Bio-rad) with the following parameters: 200 V, 110 mA for 5 min. The gel was stained with Coomassie blue staining (Bio-Safe™ Coomassie, Bio-Rad, France) while shaking on an orbital shaker for 60 min, after which the gel was washed twice with 100 mL of Milli-Q water.

The protein band visualized by Coomassie blue staining was excised from the gel, cut into small pieces (≈ 2 mm slice), and transferred to 1.5-mL microcentrifuge tubes. The gel pieces were rinsed twice with 50 mM NH_4HCO_3 and 50% CH_3CN and dried at room temperature. The gel pieces were discolored by washing twice with 50 mM NH_4HCO_3 and 50% CH_3CN and dried at room temperature. The proteins trapped in a gel slice were first reduced in 10 mM of DTT at 56 °C for 30 min, then they were alkylated using 50 mM of iodoacetamide in the dark for 45 min. The in-gel digestion was performed in 50 mM ammonium bicarbonate pH 8.0, and the quantity of sequencing grade modified trypsin (Promega, sequencing grade) was 0.1 µg per sample. Digestion was carried out at 37 °C overnight. The resulting peptides were extracted in several steps: the supernatant of trypsin hydrolysis was transferred to a new tube, and the gel slices were first extracted with the solution of 50 mM CH_3CN, 0.5% Trifluoroacetic acid TFA in water and then using a pure solution of CH_3CN. The gel slices were incubated for 15 min at room temperature for each extraction while shaking. The supernatants of each extraction were pooled with the original trypsin digest supernatant and dried for 1 h in a Speed-Vacuum concentrator. The peptides were then resuspended in 15 µL of precolumn loading buffer (0.08% trifluoroacetic acid (TFA) and 2% acetonitrile (ACN in water) before LC–MS/MS analysis.

LC–MS/MS analysis

The analysis of digested peptide was performed on an Ultimate 3000 RSLCnano system (Thermo Fisher Scientific, France) coupled to an Orbitrap Fusion Lumos Tribrid Mass Spectrometer (Thermo Fisher Scientific ; PAPPSO proteomic platform, INRA, Jouy-en-Josas). Tryptic peptide mixtures (4 µl) were loaded at 20 µl/min flow rate onto a desalting precolumn Pepmap C18 (0.3 × 5 mm, 100Å , 5µm, Thermo Fisher Scientific, France). After 4min, the precolumn was connected to the separating nanocolumn Pepmap C18 (0.075 × 50 cm, 100 Å, 2 µm, Thermo Fisher Scientific, France) and the peptides were eluted with a two-step gradient of buffer B (80% acetonitrile, 0.1% formic acid) in buffer A (2% acetonitrile, 0.1% formic acid) during 65 min. Ionization (1.6 kV ionization potential) and capillary transfer (275 °C) were performed with a liquid junction and a capillary probe (SilicaTip™ Emitter, 10 µm, New Objective). Peptide ions were analyzed using Xcalibur 3.1.66.10. The machine settings were as follows: (1) full MS scan in Orbitrap (scan range = 400 m/z –1,500 m/z), (2) MS/MS using CID (35% collision energy) in Orbitrap, (3) resolution = 120 000 and (4) fragmentation cycle TopN: Top Speed.

Processing and bioinformatics analyses

The raw files produced under Xcalibur were first converted into mzXML files with MS Convert (ProteoWizard v 3.0.8934). In a second step, protein identification was performed with X!Tandem Piledriver (v 2015.04.01.1) and X! Tandem Pipeline (v 3.4.2 "Elastine Durcie") against a protein database of *L. carnosus* (formerly *L. piscium*) protein database (NCBI, 6937 proteins downloaded March, 13th, 2017) and *L. monocytogenes* (UniprotKB, proteins downloaded March, 13th, 2017), and also against a classical proteomic contaminant database. The X!Tandem search parameters were trypsin specificity with three missed cleavages and variable oxidation states of methionine. Semi-tryptic peptide detection was included by mass tolerance of 10 ppm and a fragment mass tolerance of 0.5 Da. The identified proteins were filtered as follows: (1) peptide $E < 0.01$ with a minimum of 2 peptides per protein and (2) a protein $E < 10^{-4}$.

Detection of protein abundance changes using Label-free quantification

After analysis of each independent biological replicate, a final dataset containing only proteins present in all three datasets was generated. Protein abundance was quantified using spectral abundance factor (NSAF) as described before[48,49]. The NSAF for a given protein *k* is defined as follows:

$$(NSAF)_k = \frac{(SC/L)_k}{\sum_{i=1}^{N} (SC/L)_i}$$

Here, SC represents the number of spectral counts identified for protein *k*, L is the length of protein *k* in amino acid, and the sum is taken over all *N* proteins in the experiment with at least two valid spectral counts out of the three biological experiments. For the statistical analysis of the dataset, the natural log of each NSAF value was calculated, and two-tailed unpaired t-tests were performed to compare the ln(NSAF) from the three biological replicates of the coculture condition against the ln(NSAF) from the three biological replicates of the monoculture condition. Proteins showing differential abundance between the two culture conditions were filtered based on the following criteria: Log2 fold change (NSAF coculture / NSAF monoculture) greater than + 2 or less than – 2 and *p*-value less than 0.05. Statistical analysis was performed using XLSTAT software (version 2018.4). Statistical analysis was conducted using XLSTAT software (version 2018.4).

In silico predictions of protein subcellular localization and function

Prediction of subcellular localization was obtained using the web-server predictors psortb (https://www.psort.org/psortb/)[50]. The molecular function (MF) and biological process (BP) classification of the identified proteins were performed by the Blast2GO software (http://www.blast2go.org/)[51] and BlastKOALA (https://www.kegg.jp/blastkoala/)[52].

LYSO amino acid sequence from the *L. carnosus* (formerly *L. piscium)* CNCM I-4031 genome (SCA91560) was analyzed with Interproscan a tool available at the (https://www.ebi.ac.uk/interpro/) and SMART (Simple Modular Architecture Research Tool) is a web resource (http://smart.embl.de/) providing functional analysis and extensive annotation of protein domains and important sites[53,54]. The presence of signal peptides and transmembrane regions was predicted by using SignalP 5.0 server (http://www.cbs.dtu.dk/services/SignalP/index.php)[55].

RNA expression analysis of the differentially expressed cell-surface proteins by RT-qPCR

The cultures were grown in triplicate at 26 °C for 25 h under the conditions previously described. Before RNA isolation, the bacterial samples were directly treated with RNA-protect Bacteria Reagent (Qiagen) to stabilize RNA and were centrifuged at 5000g for 5 min at 4 °C to collect the bacterial cells. The bacterial pellets were immediately frozen in liquid nitrogen and stored at – 80 °C until RNA extraction. The frozen bacterial pellets were subjected to chemical and mechanical disruption using a Lysis buffer (TE 30mM, EDTA 1mM, pH8, Lysozyme 15mg/mL, 20µl Proteinase K) for 10 min at room temperature and a bead beater (FastPrep, Thermo Fisher Scientific) run at a frequency of 5.5 m/s, for 40s, with beads (Matrice de lyse B, MP Biomedicals™,Thermo Fisher Scientific). The total RNA was then extracted using the RNeasy Plant Mini Kit (Qiagen, Germany) according to the manufacturer's instructions. The quality of the obtained RNA was verified by the Nanodrop method and confirmed by electrophoretic analysis on RNA nano. The valid Bacterial RNA was reverse transcribed into cDNA using the iScript™ cDNA synthesis kit (Bio-rad). The expression levels of the two significant MA cell-surface proteins (LYSO and PLY) were examined. The specific primer sets to *L .carnosus* designed for amplification of reference genes (*rpoB* and *recA*) and genes encoding for the MA cell surface proteins are shown in Supplementary Table S2. Relative gene expression was measured by real-time PCR using the SYBR Green Supermix (Bio-rad) and the CFX Real-Time PCR Detection System (Bio-rad). Each experimental group contained two technical replicates. Deionized water was used as a negative control. Relative quantification was performed using the $2^{-\Delta\Delta Ct}$ method, where $\Delta\Delta Ct = (Ct_{target} - Ct_{reference\ gene})$ in coculture – $(Ct_{target} - Ct_{reference\ gene})$ in monoculture. All the quantifications of target genes were performed in triplicate and were represented as an averaged value ± SD. The difference between the two groups was analyzed using the two-tailed Student *t*-test. $P < 0.05$ was considered significant, with * indicating $P < 0.05$ and ** indicating $P < 0.01$.

Molecular cloning

For insertional inactivation of *LYSO* gene, a 461 bp internal fragment of the *LYSO* coding sequence (594 pb) and 1206 bp of erythromycin resistance cassette were amplified by PCR from the chromosomal DNA of *L. carnosus* CNCM-I 4031 and plasmid pHSP02 (Addgene), respectively, using the primer pairs listed in Supplementary Table S2. All PCR products were amplified using Q5® High-Fidelity 2X Master Mix (NEB) and purified using the PCR & DNA Cleanup kit (NEB). Using the Gibson NEB Assembly Kit, the internal fragment and the erythromycin resistance cassette were assembled and ligated into digested puC19 at the EcoRI-HindIII restriction site. Next, the Gibson assembly reaction mixture is transformed into chemically competent *E. coli* DH5α cells. Colony PCR and plasmid miniprep followed by restriction digestion were used to screen for recombinant plasmid containing a desired insert. The insert and the resulting integrative plasmid pUC:emR:*LYSO* were validated by Sequencing at Eurofins Genomics.

For recombinant expression, the sequence encoding for truncated *LYSO* protein (residues between 25 and 197) that lacks the native signal peptide was codon-optimized for *E. coli* using the GeneOptimizer® expert software. The designed sequence gene was synthesized by GeneArt Gene Synthesis Service (ThermoFisher Scientific®) and then was cloned into a pET100/D-TOPO expression vector (ThermoFisher Scientific®), resulting in the expression plasmid pET100::$LYSO_{25\text{-}197}$ (Fig. S5). This expression vector produces N-terminal 6 His-tag $LYSO_{25\text{-}197}$ protein in the cytoplasmic compartment of *E.coli*.

For the periplasmic expression vector pET-22b::$LYSO_{25\text{-}197}$, PCR product of 6xHis- $LYSO_{25\text{-}197}$ amplified from pET100::$LYSO_{25\text{-}197}$ was subsequently cloned to pET22b (+) (containing the N-terminal pelB sequence) using Gibson assembly (Fig. S6). All primers and plasmids used for cloning are listed in the Supplementary Table S2. The lines of all constructs used in this study were confirmed by DNA sequencing to ensure the absence of point mutations in the cloned genes using the Eurofins Genomics sequencing service.

E. coli toxicity assay

For comparison of cytoplasmic versus periplasmic toxicity of $LYSO_{25–197}$. Overnight cultures of *E. coli* Lemo 21 (DE3) carrying empty plasmid (pET-22b or pET100), a plasmid expressing $LYSO_{25–197}$ protein for cytoplasmic (pET100::$LYSO_{25\text{-}197}$) or periplasmic (pET-22-*Peri-LYSO* $_{25–197}$) localization were adjusted to 1 OD_{600} and serially diluted in LB (1:10) and five µL were spotted onto LB agar (1.5%) containing 100 µg/mL ampicillin with or without 400 µM of IPTG and incubated at 37 °C. Images were acquired after 24 h.

For growth curves, overnight cultures of *E. coli* Lemo 21 (DE3) containing empty pET-22b or pET-22b::$LYSO_{25\text{-}197}$ were sub-inoculated to an optical density at 600 nm (OD_{600}) of 0.01 in LB medium supplemented with 100 µg/mL ampicillin and grown at 37 °C. Cultures were induced with 400 µM IPTG after 2h45 of growth. Cell growth was tracked for eight hours by measuring the OD_{600} every 15 min. The results represented three independent experiments' mean ± standard deviations (error bars).

Microscopy

For time-lapse microscopy, *E. coli* Lemo 21 (DE3) carrying the pET-22-*Peri-LYSO* $_{25–197}$ plasmid was cultivated in LB medium with ampicillin until reaching an OD_{600} of 0.4–0.5. Five microliters were then placed on 1% LB agar pads supplemented with ampicillin, with or without 400 µM of IPTG. The bacterial growth was observed in a heated chamber at 37 °C. Images were captured every 15 min for 4 h using brightfield illumination on a Nikon Ti2 microscope equipped with an ORCA Flash 4.0 CMOS camera and an HP APO 1.49 N.A. 100 × oil immersion objective. The images were analyzed using NiS-Elements software (version 5.40.01, Nikon Instruments Inc., Nikon Europe B.V.).

Inactivation of the LYSO Gene in *L. carnosus* CNCM-I 4031 by Suicide Vector

The integrative plasmid pUC:em^R:*LYSO* isolated from an *E. coli* 5α transformant was used to transform *L. carnosus* CNCM-I 4031 by electroporation as was essentially done as described before[56,57] with the following modification.

L. carnosus CNCM-I 4031 colony was inoculated in 5 ml of GM17 (M17 medium containing 0.5% glucose) and cultured at 26 °C for eight hours. The preculture was used to inoculate at 1% a G-GM17 medium (M17 medium containing 0.5% glucose and 2,5% glycine) and grown at 26 °C to an OD600 between 0.2 and 0.3. Subsequently, the culture was centrifuged at 6,000 g for 10 min at 4 °C, and the collected pellet was washed twice. The cells were first washed with 1 volume ice-cold solution A (0.5 M sucrose and 10% glycerol) and centrifuged. Next, The pellet was resuspended in 0.5 volume ice-cold solution A supplemented with 50 mM Na-EDTA, pH 7.5, and incubated for 15 min on ice before centrifugation. Finally, the last wash was done with a 0.25-volume solution. In each step, the pellet was collected by centrifugation at 6,000 × g for 10 min at 4 °C and was resuspended by scraping thoroughly. After the last wash, the pellet was resuspended in 0.01 volume ice-cold solution A, and aliquots of 50 µl were flash-frozen with nitrogen and stored at – 80 °C until use. For electroporation, a 50 µl aliquot of thawed electrocompetent CNCM-I 4031 cells was mixed with 150 ng of pUC:emR:*LYSO* plasmid in an ice-cooled electroporation cuvette (2 mm electrode gap) and exposed to a single electrical pulse of 2 kV field strength, 25 µF capacitance, and 200 Ohm resistance using a Gene Pulser XcellTM (Bio-Rad Laboratories, Richmond, CA, USA). Immediately after discharge, 950 µL of ice-cold GM17 containing 20 mM $MgCl_2$ and two mM $CaCl_2$ was added to the cuvette, which was left on ice for 10 min and then incubated at 26 °C for 2.5 h. Finally, transformed cells were plated and fixed for 72 h at 26 °C on GM17 medium containing 1.5% agar supplemented with 10 µg·ml-1 erythromycin to select CNCM-I 4031 mutants harboring the inserted pUC:emR:*LYSO*. Vector insertion into the chromosome and disruption of the *LYSO* coding sequence were verified by DNA sequencing of PCR products generated using the primers listed in Supplemental file 2 (for more information, see Fig. S4). In addition, insertion stability was verified after three independent cultures in GM17 and MSMA media without erythromycin. *L. carnosus* WT and Δ*LYSO* growth was monitored in a BHI medium with an initial concentration of 10^6 CFU/ml. 100µL of bacterial suspension was placed in a well of a 96-well plate in triplicate. TECAN monitored growth for 24 h at 26 °C, with $OD_{600\ nm}$ readings taken every 30 min.

Bacterial competition experiments

Coculture assays were performed as previously described above with some modifications. The experiments to assess the contact dependence of growth inhibition were done in a Costar six-well polystyrene culture plate (Corning) carrying transwell inserts with a porous membrane (BD Falcon). The membrane contained 0.22 µm pores to restrict the passage and the contact between the inhibitor and target bacteria cells. For coculture without cell–cell interaction, *L. carnosus* (≈ 10^6 CFU/mL) was added to the transwell insert, and *L. monocytogenes* (≈ 10^3 CFU/mL) was added to the lower chamber (well). For coculture with cell-to-cell contact, *L. carnosus* (≈ 10^6 CFU/mL) and *L. monocytogens* (≈ 10^3 CFU/mL) were cultivated in fresh MSMA medium in the same well to allow mixing of both bacteria populations. Plates were covered with a lid and incubated for 25 h at 26 °C. As reported above, viable inhibitor and target cell counts were quantified as colony-forming units per millilitre by plating in selective growth conditions.

Expression and purification of His-tagged LYSO

The recombinant vector pET100::$LYSO_{25\text{-}197}$ was transformed into *E. coli* Lemo21 (DE3) competent cells (NEB, C2528J) according to manufacturer specifications. The Lemo21 (DE3) cells harbouring the plasmid were grown under agitation (250 rpm) at 37 °C in LB medium (Invitrogen, 12780052) containing 100 µg/ml ampicillin and 34 µg/ml chloramphenicol. When bacterial cells reached an OD600 nm of 0.5, 40 µM of IPTG (Thermo scientific®) was added to induce protein expression. Cultures were induced for approximately 4 h before being harvested by centrifugation at 6000 rpm for 10 min at 4 °C and then frozen at – 20 °C overnight. The recombinant His-tagged LYSO was expressed in the inclusion bodies (as an insoluble form), and the purification was conducted under denaturing conditions. Briefly, the cell pellets were resuspended in lysis buffer (20 mM sodium phosphate, 300 mM NaCl, 2 mM imidazole, pH 7.4) containing a denaturing agent (8M urea) and were sonicated on ice (12 cycles, 15 s ON/OFF). The lysed cells were incubated at 25 °C for 60 min and then centrifuged at 10,000 rpm for 20 min. The resulting supernatant was subjected to Immobilized metal-affinity chromatography (IMAC) using the Nickel spin column (NEBExpress® Ni Spin columns, NEB). The column was washed three times with Wash Buffer (20 mM sodium phosphate, 300 mM NaCl, 20 mM imidazole, 8M urea, pH 7.4). Then, the His-tagged T-LYSO was eluted with the Elution Buffer (20 mM sodium phosphate, 300 mM NaCl, 500 mM imidazole, 8M urea, pH 7.4). The purified protein was quantified using the BCA Protein Assay Kit (Thermo Fisher Scientific, Waltham, MA, USA) according to the manufacturer's instructions. The pure protein was stored at – 80 °C. The production and the purification of the His-tagged protein were checked by SDS-PAGE and Western blot[58,59], respectively. SDS-PAGE was performed with 12.5% (w/v) polyacrylamide separating gels. Gels were stained with Bio-Safe™ Coomassie Stain solution (Bio-rad). For Western blot assay, the proteins were separated by SDS-PAGE and transferred to nitrocellulose membrane (0,2µm) (Bio-rad) for immunoblot detection with anti-6x-His Tag mouse monoclonal Antibody (HRP) (MA1-21315, Thermo Fisher Scientific) and SuperSignal West Pico PLUS Chemiluminescent Substrate (Thermo Fisher Scientific). Pierce Prestained Protein MW Marker (26612, Life Technologies) and Precision Plus Protein™ Dual Xtra Prestained Protein Standards (1610377, Bio-rad) were used as molecular weight markers.

Zymogram analysis

The zymogram assay was used to detect cell wall hydrolase activity and was performed as described previously[60] with some modifications. Lytic activity was detected by using SDS–12.5% polyacrylamide gels containing 0.2%

(wt/vol) of *Micrococcus lysodeikticus* cells (M0508, Sigma) or autoclaved cells of *L. carnosus* or *L. monocytogenes*. After sample migration, gels were washed for 15 min in deionized H_2O and incubated for 48 h at 25 °C in Renaturing Buffer (25 mM Tris–HCl, 1% Triton X-10, pH 7,2) to allow for protein renaturation. During this step, the gels were gently shaken with three to five changes of Renaturing Buffer. Subsequently, the gels were washed in deionized H_2O, followed by staining with 0.1% Methylene Blue in 0.01% (w/v) KOH and destained in deionized H_2O. The peptidoglycan hydrolase activity on zymogram gel is identified as a clear band. Commercial lysozyme from hen egg white (Sigma) was used as a positive control for cell wall hydrolase activity. A zymogram assay control was performed in the same way as the normal zymogram, except the protein refolding step was removed[60]. Thus, after the SDS-PAGE was run, the gel was washed and immediately stained with methylene blue solution.

Data availability

All data generated or analyzed during this study are included in this published article and its supplementary information files.

Received: 14 October 2024; Accepted: 19 May 2025
Published online: 28 May 2025

References

1. Guérin, A. et al. Advanced 'omics approaches applied to microbial food safety & quality. In *Food Molecular Microbiology* 88–123 (CRC Press, 2019). https://doi.org/10.1201/9781315110110-6.
2. Elsser-Gravesen, D. & Elsser-Gravesen, A. Biopreservatives. *Adv. Biochem. Eng. Biotechnol.* **143**, 29–49 (2013).
3. Camargo, A. C., Todorov, S. D., Chihib, N. E., Drider, D. & Nero, L. A. Lactic Acid Bacteria (LAB) and their bacteriocins as alternative biotechnological tools to control listeria monocytogenes biofilms in food processing facilities. *Mol. Biotechnol.* **60**, 712–726 (2018).
4. Jordan, K. & McAuliffe, O. Listeria monocytogenes in foods. In *Advances in Food and Nutrition Research, vol. 86* 181–213 (Academic Press Inc., 2018).
5. Borges, F. et al. Contribution of omics to biopreservation: toward food microbiome engineering. *Front. Microbiol.* **13**, 456 (2022).
6. Silva, C. C. G., Silva, S. P. M. & Ribeiro, S. C. Application of bacteriocins and protective cultures in dairy food preservation. *Front. Microbiol.* **9**, 594–594 (2018).
7. Woraprayote, W. et al. Bacteriocins from lactic acid bacteria and their applications in meat and meat products. *Meat Sci.* **120**, 118–132 (2016).
8. Gao, Z. et al. Inhibitory effect of lactic acid bacteria on foodborne pathogens: a review. *J. Food Prot.* **82**, 441–453 (2019).
9. Garcia, E. C. Contact-dependent interbacterial toxins deliver a message. *Curr. Opin. Microbiol.* **42**, 40–46 (2018).
10. García-Bayona, L. & Comstock, L. E. Bacterial antagonism in host-associated microbial communities. *Science* **361**, 456 (2018).
11. Werum, V., Ehrmann, M., Vogel, R. & Hilgarth, M. Comparative genome analysis, predicted lifestyle and antimicrobial strategies of *Lactococcus carnosus* and *Lactococcus paracarnosus* isolated from meat. *Microbiol. Res.* **258**, 126982 (2022).
12. Matamoros, S. et al. Psychrotrophic lactic acid bacteria used to improve the safety and quality of vacuum-packaged cooked and peeled tropical shrimp and cold-smoked salmon. *J. Food Prot.* **72**, 365–374 (2009).
13. Matamoros, S., Pilet, M. F., Gigout, F., Prévost, H. & Leroi, F. Selection and evaluation of seafood-borne psychrotrophic lactic acid bacteria as inhibitors of pathogenic and spoilage bacteria. *Food Microbiol.* **26**, 638–644 (2009).
14. Fall, P. A. et al. Sensory and physicochemical evolution of tropical cooked peeled shrimp inoculated by Brochothrix thermosphacta and Lactococcus piscium CNCM I-4031 during storage at 8°C. *Int. J. Food Microbiol.* **152**, 82–90 (2012).
15. Fall, P. A., Leroi, F., Chevalier, F., Guérin, C. & Pilet, M.-F. Protective Effect of a non-bacteriocinogenic *Lactococcus piscium* CNCM I-4031 strain against listeria monocytogenes in sterilized tropical cooked peeled Shrimp. *J. Aquat. Food Prod. Technol.* **19**, 84–92 (2010).
16. Hilgarth, M., Nani, M. & Vogel, R. F. Assertiveness of meat-borne Lactococcus piscium strains and their potential for competitive exclusion of spoilage bacteria in situ and in vitro. *J. Appl. Microbiol.* **124**, 1243–1253 (2018).
17. Saraoui, T. et al. Inhibition mechanism of Listeria monocytogenes by a bioprotective bacteria Lactococcus piscium CNCM I-4031. *Food Microbiol.* **53**, 70–78 (2016).
18. Chassaing, B. & Cascales, E. Antibacterial weapons: targeted destruction in the microbiota. *Trends Microbiol.* **26**, 329–338 (2018).
19. Russell, A. B., Peterson, S. B. & Mougous, J. D. Type VI secretion system effectors: poisons with a purpose. *Nat. Rev. Microbiol.* **12**, 137–148 (2014).
20. Souza, D. P. et al. Bacterial killing via a type IV secretion system. *Nat. Commun.* **6**, 6453–6453 (2015).
21. Willett, J. L. E., Gucinski, G. C., Fatherree, J. P., Low, D. A. & Hayes, C. S. Contact-dependent growth inhibition toxins exploit multiple independent cell-entry pathways. *Proc. Natl. Acad. Sci. U.S.A.* **112**, 11341–11346 (2015).
22. Jamet, A., Charbit, A. & Nassif, X. Antibacterial toxins: gram-positive bacteria strike back!. *Trends Microbiol.* **26**, 89–91 (2018).
23. Kobayashi, K. Diverse LXG toxin and antitoxin systems specifically mediate intraspecies competition in Bacillus subtilis biofilms. *PLoS Genet.* **17**, e1009682 (2021).
24. Meza-Torres, J. et al. Listeriolysin S: a bacteriocin from Listeria monocytogenes that induces membrane permeabilization in a contact-dependent manner. *Proc. Natl. Acad. Sci.* **118**, e2108155118 (2021).
25. Koskiniemi, S. et al. Rhs proteins from diverse bacteria mediate intercellular competition. *Proc. Natl. Acad. Sci.* **110**, 7032–7037 (2013).
26. Vollmer, W., Joris, B., Charlier, P. & Foster, S. Bacterial peptidoglycan (murein) hydrolases. *FEMS Microbiol. Rev.* **32**, 259–286 (2008).
27. Vermassen, A. et al. Cell wall hydrolases in bacteria: insight on the diversity of cell wall amidases, glycosidases and peptidases toward peptidoglycan. *Front. Microbiol.* **10**, 14 (2019).
28. Simons, A., Alhanout, K. & Duval, R. E. Bacteriocins, antimicrobial peptides from bacterial origin: overview of their biology and their impact against multidrug-resistant bacteria. *Microorganisms* **8**, 639 (2020).
29. Bastos, M., Coutinho, B. G. & Coelho, M. L. V. Lysostaphin: a staphylococcal bacteriolysin with potential clinical applications. *Pharmaceuticals* **3**, 1139–1161 (2010).
30. Lahiri, D. et al. Bacteriocin: a natural approach for food safety and food security. *Front. Bioeng. Biotechnol.* **10**, 123 (2022).
31. Nilsen, T., Nes, I. F. & Holo, H. Enterolysin A, a Cell Wall-Degrading Bacteriocin from Enterococcus faecalis LMG 2333. *Appl. Environ. Microbiol.* **69**, 2975–2984 (2003).
32. Kurushima, J., Hayashi, I., Sugai, M. & Tomita, H. Bacteriocin Protein BacL1 of Enterococcus faecalis Is a Peptidoglycan d-Isoglutamyl-l-lysine Endopeptidase*. *J. Biol. Chem.* **288**, 36915–36925 (2013).
33. Hickey, R. M., Twomey, D. P., Ross, R. P. & Hill, C. Production of enterolysin A by a raw milk enterococcal isolate exhibiting multiple virulence factors. *Microbiol. (Reading)* **149**, 655–664 (2003).

34. García-Bayona, L., Guo, M. S. & Laub, M. T. Contact-dependent killing by Caulobacter crescentus via cell surface-associated, glycine zipper proteins. *Elife* **6**, 112 (2017).
35. Claverys, J.-P. & Håvarstein, L. S. Cannibalism and fratricide: mechanisms and raisons d'être. *Nat. Rev. Microbiol.* **5**, 219–229 (2007).
36. Ikryannikova, L. N., Kurbatov, L. K., Soond, S. M. & Zamyatnin, A. A. Harnessing the potential of killers and altruists within the microbial community: a possible alternative to antibiotic therapy?. *Antibiotics Basel* **8**, 230 (2019).
37. Tran, H. K. R., Grebenc, D. W., Klein, T. A. & Whitney, J. C. Bacterial type VII secretion: an important player in host-microbe and microbe-microbe interactions. *Mol. Microbiol.* **115**, 478–489 (2021).
38. Whitney, J. C. et al. A broadly distributed toxin family mediates contact-dependent antagonism between gram-positive bacteria. *Elife* **6**, 145 (2017).
39. Teh, W. K. et al. Characterization of TelE, a T7SS LXG effector exhibiting a conserved C-terminal glycine zipper motif required for toxicity. *Microbiol. Spectrum* **11**, e01481-e1523 (2023).
40. Alcock, F. & Palmer, T. Activation of a bacterial killing machine. *PLoS Genet* **17**, e1009261 (2021).
41. Basler, M., Ho, B. T. & Mekalanos, J. J. Tit-for-tat: type VI secretion system counterattack during bacterial cell-cell interactions. *Cell* **152**, 884–894 (2013).
42. Kennedy, N. W. & Comstock, L. E. Mechanisms of bacterial immunity, protection, and survival during interbacterial warfare. *Cell Host Microbe* **32**, 794–803 (2024).
43. DeHart, H. P., Heath, H. E., Heath, L. S., LeBlanc, P. A. & Sloan, G. L. The lysostaphin endopeptidase resistance gene (epr) specifies modification of peptidoglycan cross bridges in *Staphylococcus simulans* and *Staphylococcus aureus*. *Appl. Environ. Microbiol.* **61**, 1475–1479 (1995).
44. Beukes, M. & Hastings, J. W. Self-protection against cell wall hydrolysis inStreptococcus milleri NMSCC 061 and analysis of the millericin B Operon. *Appl. Environ. Microbiol.* **67**, 3888–3896 (2001).
45. Briers, Y., Klumpp, J., Schuppler, M. & Loessner, M. J. Genome sequence of Listeria monocytogenes Scott A, a clinical isolate from a food-borne listeriosis outbreak. *J. Bacteriol.* **193**, 4284–4285. https://doi.org/10.1128/JB.05328-11 (2011).
46. Marché, L. et al. Complete genome sequence of Lactococcus piscium CNCM I-4031, a bioprotective strain for seafood products. *Genome Announce.* **5**, 456 (2017).
47. Gitton, C. et al. Proteomic signature of *Lactococcus lactis* NCDO763 cultivated in milk. *Appl. Environ. Microbiol.* **71**, 7152–7163 (2005).
48. Zybailov, B. et al. Statistical analysis of membrane proteome expression changes in *Saccharomyces cerevisiae*. *J. Proteome Res.* **5**, 2339–2347 (2006).
49. Paoletti, A. C. et al. Quantitative proteomic analysis of distinct mammalian Mediator complexes using normalized spectral abundance factors. *Proc. Natl. Acad. Sci. U. S. A.* **103**, 18928–18933 (2006).
50. Yu, N. Y. et al. PSORTb 3.0: improved protein subcellular localization prediction with refined localization subcategories and predictive capabilities for all prokaryotes. *Bioinformatics* **26**, 1608–1615 (2010).
51. Conesa, A. et al. Blast2GO: a universal tool for annotation, visualization and analysis in functional genomics research. *Bioinformatics* **21**, 3674–3676 (2005).
52. Kanehisa, M., Sato, Y. & Morishima, K. BlastKOALA and GhostKOALA: KEGG tools for functional characterization of genome and metagenome sequences. *J. Mol. Biol.* **428**, 726–731 (2016).
53. Mitchell, A. et al. The InterPro protein families database: the classification resource after 15 years. *Nucleic Acids Res.* **43**, D213–D221 (2015).
54. Letunic, I. & Bork, P. 20 years of the SMART protein domain annotation resource. *Nucleic Acids Res.* **46**, D493–D496 (2018).
55. Almagro Armenteros, J. J. et al. SignalP 5.0 improves signal peptide predictions using deep neural networks. *Nat. Biotechnol.* **37**, 420–423 (2019).
56. H, H. & If, N. High-Frequency transformation, by electroporation, of lactococcus lactis subsp. cremoris grown with glycine in osmotically stabilized media. *Appl. Environ. Microbiol.* **55**, 145 (1989).
57. Wells, J. M., Wilson, P. W. & Le Page, R. W. Improved cloning vectors and transformation procedure for Lactococcus lactis. *J. Appl. Bacteriol.* **74**, 629–636 (1993).
58. Laemmli, U. K. Cleavage of structural proteins during the assembly of the head of bacteriophage T4. *Nature* **227**, 680–685 (1970).
59. Towbin, H., Staehelin, T. & Gordon, J. Electrophoretic transfer of proteins from polyacrylamide gels to nitrocellulose sheets: procedure and some applications. *Proc. Natl. Acad. Sci. U.S.A.* **76**, 4350–4354 (1979).
60. Escobar, C. A. & Cross, T. A. False positives in using the zymogram assay for identification of peptidoglycan hydrolases. *Anal. Biochem.* **543**, 162–166 (2018).

Acknowledgements

This work was financially supported by the COM-BACT and PULSAR LYSO projects, funded by the Région des Pays de la Loire, France. The authors thank Monique Zagorec and Christine Delbarre-Ladrat for their assistance in conceptualization, and Hakima Lakhal and Ombeline Guiguin for their contributions to the experimental work. They also thank Biogenouest, the Western France network of life sciences and environmental technology core facilities supported by the Conseil Régional des Pays de la Loire, for their support of APEX.

Author contributions

MFP, FL, and JB supervised the project. RT, MFP, DP, and FL contributed to conceptualization. RT, MFP, SR, MH, HL, and OG conducted the experiments. LD supervised and analyzed the microscopic experiments, and VM supervised the proteomic experiments. RT, SR, and MFP analyzed the results. RT and MFP wrote the manuscript. All authors reviewed the manuscript.

Competing interests

The authors declare no competing interests.

Additional information

Supplementary Information The online version contains supplementary material available at https://doi.org/10.1038/s41598-025-03177-3.

Correspondence and requests for materials should be addressed to M.-F.P.